JTTEE5 15:422-430
DOI: 10.1361/105996306X124437
1059-9630/$19.00 © ASM International

Peer Reviewed

Effect of Processing Conditions on Porosity Formation in Cold Gas Dynamic Spraying of Copper

Saden H. Zahiri, Darren Fraser, Stefan Gulizia, and Mahnaz Jahedi

(Submitted October 5, 2005; in revised form March 15, 2006)

The cold gas dynamics process is a promising low-temperature spray process in which particles are accelerated in a supersonic flow before impacting with substrate to be coated. In this study the effect of spray temperature, spray pressure, and particle size on porosity formation in cold spray coatings are investigated. Results show that an increase in spray temperature and a decrease in particle size lead to a decline in volume fraction of porosity. Furthermore, particle velocity and particle temperature are determined to be the significant parameters for elimination of porosity. A model is proposed for estimation of the volume fraction of porosity for alloy of this study.

Keywords cold gas dynamic spray, copper, Mach, particle, porosity

1. Introduction

Cold gas dynamic spray (cold spray) is a surface coating technology in which small particles in solid state are accelerated to high velocities (normally above 500 m/s) in a supersonic gas jet and deposited on the substrate material. Cold spray is a direct-deposition process capable of combining many dissimilar materials in the production of a single coating. In contrast to thermal spray processes, the process does not use a heat source but rather kinetic energy of the particles to implement bonding through plastic deformation upon impact with substrate. This provides a unique advantage for cold spray to be exploited for temperature-sensitive processes such as oxygen-sensitive, phase-sensitive, amorphous, and nanostructure materials. The mechanism for metallic bonding achieved through cold spray has been compared with explosive welding in which (at a certain velocity upon impact) thin films on the particles surfaces are ruptured generating a direct interface (Ref 1-3).

In general, cold spray exhibits two common features in the as-deposited condition, a rough (sandpaper-like) surface and a structure with inherent porosity (Ref 4-7). However, presence of porosity limits utilization of the cold spray process in many industrial applications that demand high density, high thermal conductivity, and postspray machining (e.g., mirror-finish surface quality). In a recent study, Steenkiste and Smith (Ref 7) have shown that an increase in particle velocity leads to a decline in volume fraction of porosity and improvement in adhesion of cold sprayed copper (Cu). However, the effect of cold spray parameters such as temperature and pressure on porosity formation has not been systematically studied. This study aims to identify the processing conditions that lead to control of porosity formed through the cold spray process. The results show that particle velocity, particle temperature, and particle size distribution are the most important processing conditions that affect porosity formation in the coatings of this study.

Saden H. Zahiri, Darren Fraser, Stefan Gulizia, and **Mahnaz Jahedi,** CSIRO Manufacturing and Infrastructure Technology, Gate 5, Normanby Road, Clayton, Vic. 3168, Australia. Contact e-mail: saden.zahiri@csiro.au.

2. Experimental

The effect of processing conditions on porosity formation in cold sprayed pure Cu on aluminum (Al) substrate was investigated utilizing a commercially available CGT cold spray system (CGT Technologies, Munich, Germany) (Fig. 1). Copper was chosen as the coating material due to the broad application in current cold spray industry. Copper coating was formed by exposing an Al substrate to a high-velocity stream of solid Cu phase particles that had been accelerated by a supersonic jet of nitrogen gas at a temperature ranging from 300 to 640 °C (Fig. 1). Nitrogen gas at an elevated pressure range of 2 to 3 MPa (290 to 435 psi) was introduced to a system containing a gas heater and powder feeder vessel. Heating of the pressurized gas was established electrically.

The high-pressure and high-temperature gas was introduced into a converging diverging (Laval) type nozzle (attached to a robot) wherein compression through the nozzle throat followed by expansion to atmospheric pressure resulted in a supersonic flow condition and cooling of the gas stream (Fig. 1). Temperature of the gas was measured utilizing a thermocouple located in the converging (stagnation) section of the nozzle. Similarly, a pressure sensor recorded the gas pressure in the converging part of the nozzle. The powder feedstock was introduced at 120 g/min on the high-pressure side of the nozzle. Particles were delivered by a precision metering device, which also remained at the elevated pressure of the manifold. The distance between the tip of the nozzle and the specimen (standoff) for processing conditions given in Table 1 was 25 mm, and traverse speed of the robot was 100 mm/min. The cold spray system was located within an enclosure to reduce noise level to below 90 dB.

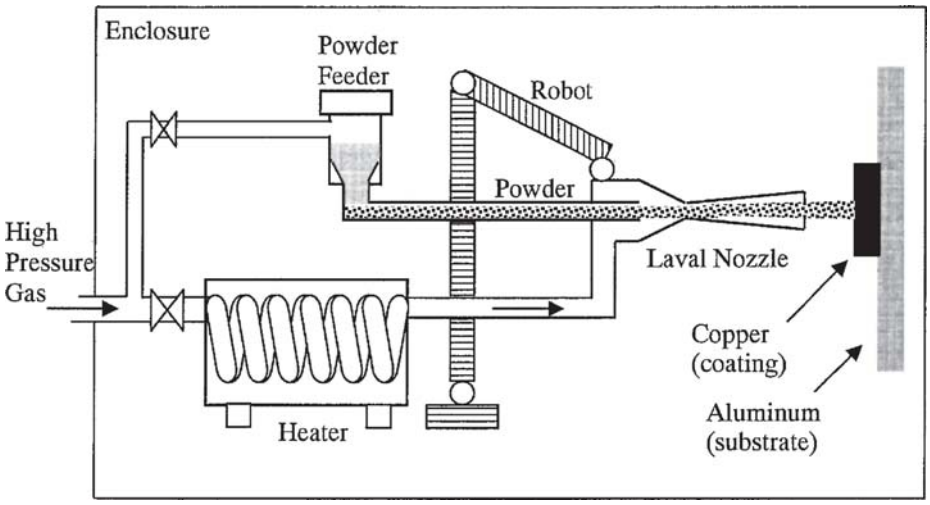

Fig. 1 Schematic representation of cold spray system used in this study

Table 1 Processing conditions for copper deposition in this study

Sample	Gas temperature, °C	Pressure, MPa, ×10 bar	Average particle size, μm
A	300	3	18
B	420	3	18
C	630	3	18
D	630	2	18
E	300	3	28

Specimens were cut and mounted from the cross section of the Cu-coated Al plates. Samples were polished (using an automated Struers [Struers GmbH, Germany] RotoPol-22 polishing machine) with 1000, 2000, and 4000 grit sand papers for 2 min. This was followed by 15, 3, and 1 μm diamond polishing. Colloidal SiO_2 (OP-S) was used for final polishing. A small force (12 N) was applied to prevent particle ejection from the specimen surface. An Olympus PMG3 (Olympus Corp., Tokyo, Japan) microscope was used for microstructural observation. Some specimens were etched in a diluted ferric chloride to study splat and porosity formed through the cold spray process. Polished (unetched) samples were prepared for image analysis in which dark areas (representing porosity) scattered in a bright matrix. ImageTool (UTHSCSA Image Tool, TX) software was used to estimate the volume (area) fraction of porosities for at least 10 random images for each experiment in Table 1. To study the effect of particle size and particle size distribution on porosity formation, two types of powders were chosen. Powder I with average particle size of 18 μm and powder II with average particle size of 28 μm were examined for a range of spray temperature and pressure (Table 1). Powder II had a larger particle size distribution compared with powder I (Fig. 2). The particle size distribution was quantified using a Malvern Mastersizer (Malvern Instruments Ltd., Worcestershire, UK) particle analyzer. The average particle size ($D_{ave.}$) was determined from results in Fig. 2 and Eq 1:

$$D_{ave} = \frac{\sum (D_p)(V)}{\sum (V)} \quad \text{(Eq 1)}$$

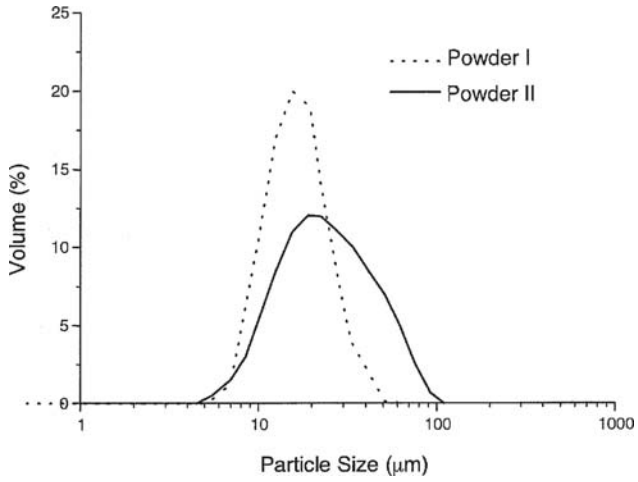

Fig. 2 Particle size distribution for powder I and powder II used in this study

where D_p is the particle size corresponding to the volume V (%) in the distribution function plot.

X-ray microdiffraction analysis was performed to examine oxide formation in the coatings. This was achieved using a Bruker (Bruker ASX, Karlsruhe, Germany) GADDS (general area detector diffraction system) x-ray microdiffractometer. The GADDS instrument was operated at 40 kV, 40 mA, with Cu Kα radiation collimated to a spot size of 500 μm for a count time of 1000 s per analysis. Two-dimensional diffraction data were recorded and converted to conventional x-ray diffraction (XRD) patterns by chi-integration around the intersected Debye cones. Crystalline phases were identified using the ICDD-JCPDS powder diffraction database and the Bruker XRD search match program EVA. This analysis enabled the identification of crystalline phases contained in the samples.

3. Results

It has been proposed in earlier studies (Ref 8-10) that temperature and pressure are the most significant processing param-

eters that affect particle deposition in the cold spray process. Temperature has a prominent effect on particle velocity once Mach speed is reached. In contrast, at Mach speed, pressure influences particle acceleration. The impact of these processing parameters on porosity formation for coatings of this study are explained in this section.

3.1 Effect of Temperature

Microstructural observations show that an increase in temperature led to a decrease in volume fraction of the porosity in the coating (Fig. 3). Quantitative image analysis of the micrographs in Fig. 3 (at least 10 images for each temperature) indicates a decrease in volume fraction of porosity from 0.7% at 300 °C to 0.05% at 420 °C and 0.005% at 630 °C (Fig. 4). The calculated standard deviations for 300, 420, and 630 °C were 0.2, 2, and 10%. This decline in volume fraction of the porosities is most likely due to the large plastic deformation of the particles. This plastic deformation is achieved from the kinetic energy that is provided by velocity of the particles (Ref 11-13). Similarly, the average porosity size declined from 45 μm at 300 °C to 2 μm at 630 °C. This confirms a larger deformation for particles at high temperatures that results in a decrease in size of the voids and cavities in the coating (Fig. 5). It is worth noting that the calculated error corresponding to average porosity increased from 5 to 35% with an increase in temperature from 300 to 630 °C, which is due to a decline in porosity size. At 630 °C, the average porosity size is 2.5 μm, which is close to the maximum precision (~2 μm) of the optical microscopy used for image analysis of this study.

To determine oxide formation in the coatings of this study, XRD patterns of Cu powder and the coated Cu were compared. The results in Fig. 6(a) show high-intensity peaks at 2θ angle 43.3° (d-spacing = 2.088 Å) and 50.43° (d-spacing = 1.808 Å), which correspond to pure Cu. A similar diffraction pattern was observed from the Cu layer after deposition at 630 °C (Fig. 6b), confirming that oxidation did not occur through the coating process. These observations verify previous findings in the literature (Ref 11, 14) and a unique advantage of the cold spray process in that oxidation has been prevented due to the low-temperature operation of the process.

3.2 Effect of Pressure

The results indicate that a decrease in pressure from 3 to 2 MPa (30 to 20 bar) led to an increase in volume fraction of porosity by more than two orders of magnitude from 0.005 to 1.1% (Fig. 7a). Similarly, Fig. 7(b) shows that the average size of porosity increased significantly from 2.5 to 51 μm. These results are consistent with previous suggestions (Ref 8) that show a decline in pressure leads to a decrease in acceleration of the particles and therefore insufficient kinetic energy and shear force for a considerable plastic deformation to eliminate porosity.

3.3 Effect of Particles

Powders I and II were cold sprayed on Al substrate at 300 °C and 3 MPa (Table 1) to study the effect of average particle size and particle size distribution on porosity formation. Results in

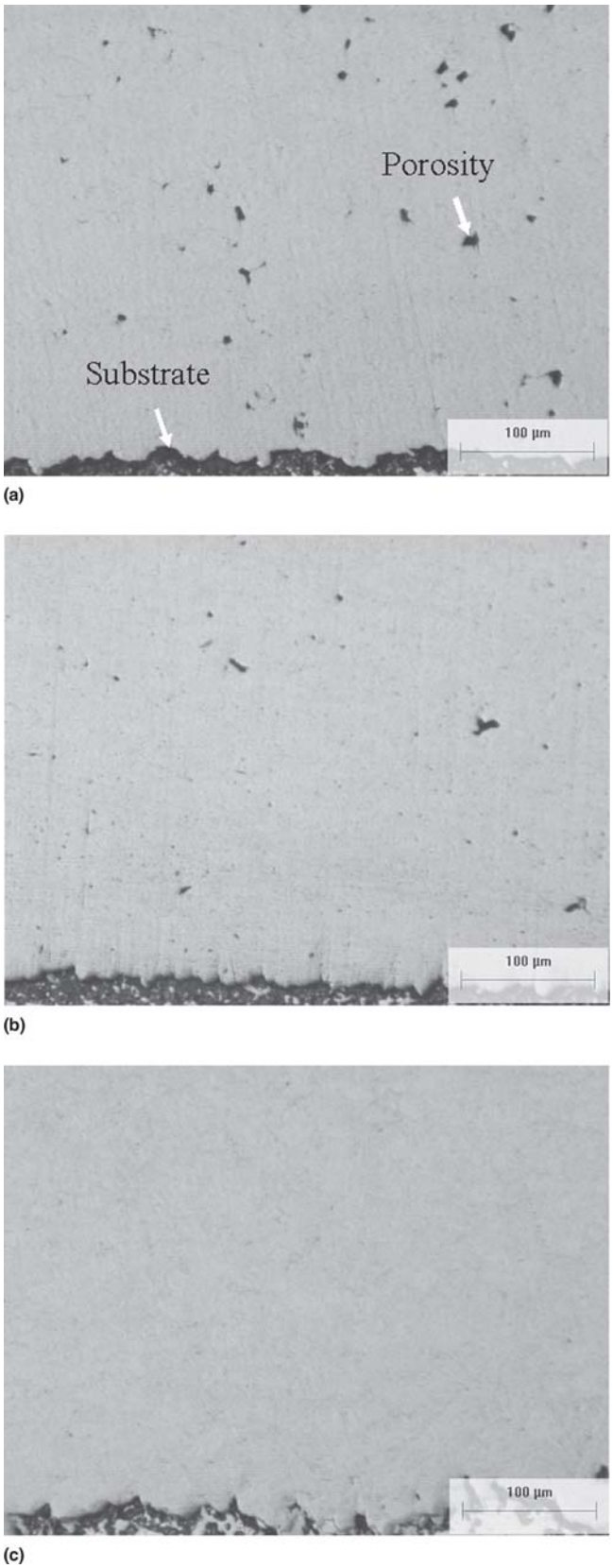

Fig. 3 Porosity formation in (unetched) cold sprayed microstructure for gas temperatures. (a) 300 °C. (b) 420 °C. (c) 630 °C

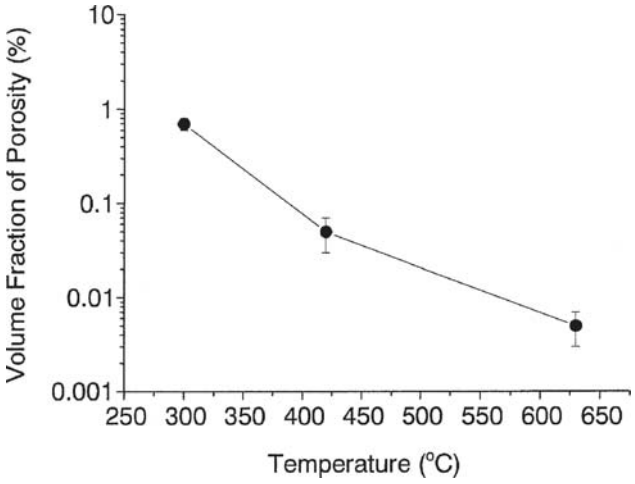

Fig. 4 Volume fraction of porosity as a function of temperature for the powder I

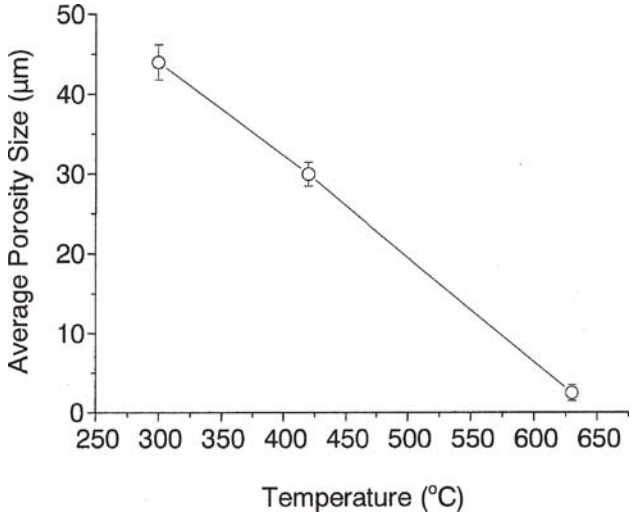

Fig. 5 Average porosity size as a function of temperature for the powder I

Fig. 8(a) indicate that the coating using powder I possessed 0.7% porosity, which is 50% less than the porosity for powder II coating. This significant reduction is most likely due to the fact that particles of powder I with 18 μm average particle size achieve a higher velocity than powder II with 28 μm average particle size. A higher velocity leads to a higher kinetic energy and a larger plastic deformation (flattening) for particles (Ref 9). Consequently, a larger deformation leads to elimination of voids produced through the cold spray process. This also contributes to a smaller average porosity size of 44 μm for powder I compared with powder II with 65 μm (Fig. 8b). Furthermore, powder I (7 to 45 μm) has particle size distribution that is narrower than powder II (7 to110 μm) particle size distribution (Fig. 2). This implies that volume fraction of large particles are considerably lower in powder I, and therefore particles of this powder gain an overall higher velocity and plastic deformation through the process.

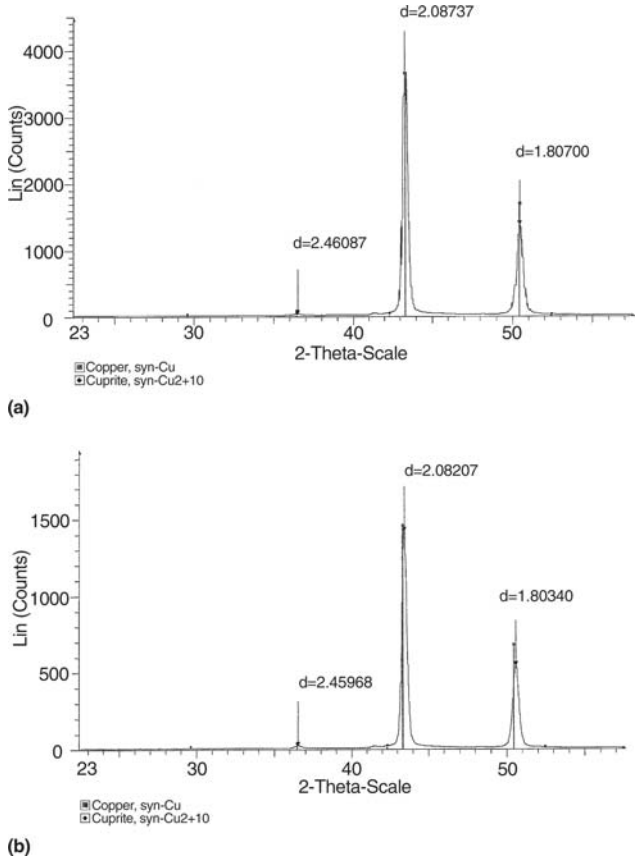

Fig. 6 X-ray diffraction plot for powder I (a) before deposition and (b) after deposition

4. Discussion

Results show that temperature, pressure, and particle size influence the volume fraction of porosity for cold spray coatings in this study. It seems that all of these processing parameters influence velocity of particles that provides the kinetic energy for particle deposition and deformation. Among these parameters, results show that spray temperature has a profound influence on porosity reduction in the coating (Fig. 3). These effects are further discussed in this section.

4.1 Effect of Temperature

It has been demonstrated that under Mach conditions temperature is the most significant parameter to achieve critical velocity for particle deposition through the cold spray process (Ref 8, 10). Results in Fig. 4 show that an increase in spray temperature from 300 to 630 °C leads to a decrease in volume fraction of porosity by two orders of magnitude. This reduction in porosity is explained by comparing particle velocity of powder I at 300 and 630 °C. Under Mach conditions, the velocity of the particles is estimated from (Ref 8):

$$V_p = (M-1)\sqrt{\frac{\gamma R T_o}{1+[(\gamma-1)/2]M^2}} \qquad \text{(Eq 2)}$$

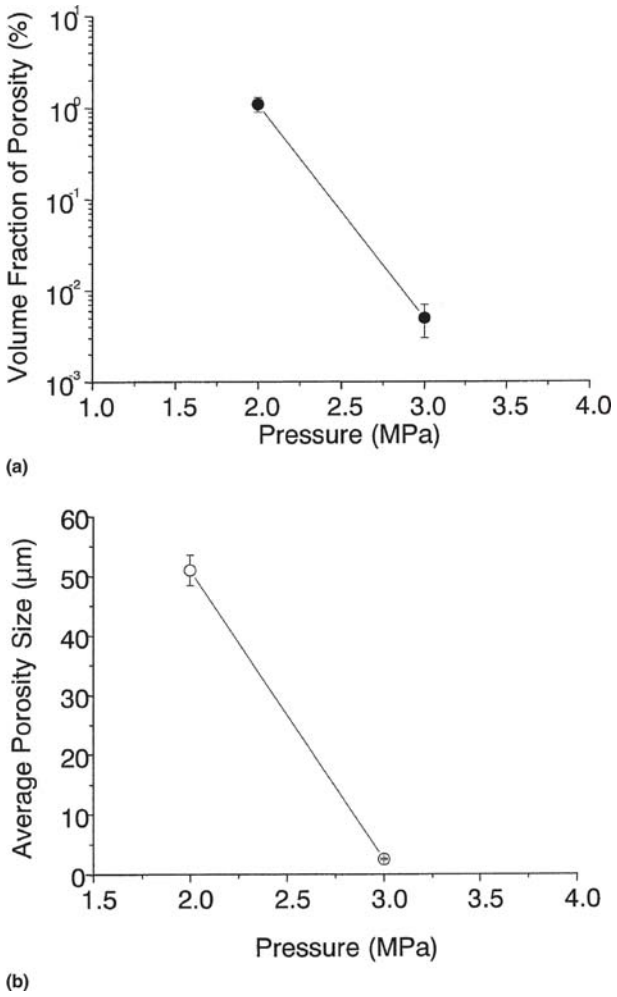

Fig. 7 Effect of pressure on (a) volume fraction of porosity and (b) average porosity size at 300 °C cold spray temperature for powder I

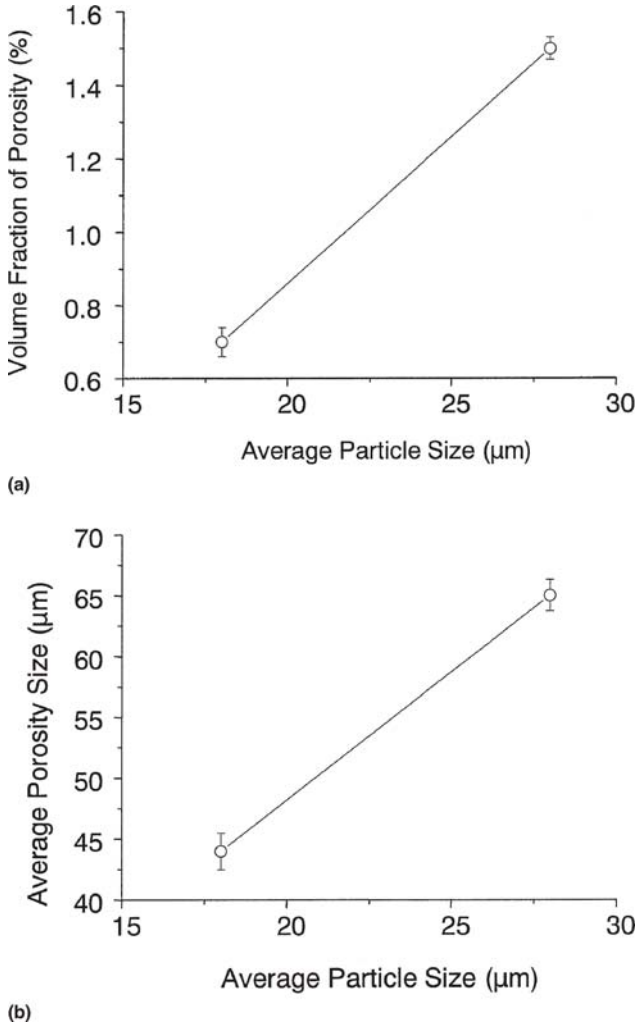

Fig. 8 Effect of average particle size of powder I (18 μm) and powder II (28 μm) on (a) volume fraction of porosity and (b) average porosity size at 3 MPa and 300 °C

where V_p is particle velocity, M is Mach number, γ is ratio of gas specific heat (for nitrogen gas in this study γ =1.4), and T_o is gas temperature. The value for M number is estimated as a function of:

$$X = \frac{xC_D A_p \rho_o}{2m} \quad \text{(Eq 3)}$$

where X is a coefficient (nondimensional distance from nozzle throat), x is the distance from throat (m), ρ_o is stagnation density (kg/m^3), C_D is drag coefficient, A_p is cross-sectional area of the particle (m^2), and m is mass of the particle (kg). Details of these calculations are explained elsewhere (Ref 8). In this study, C_D was estimated to be 0.25 and particles were assumed to be spherical. The value for m and A_p were calculated from the particle size distribution data.

For an average particle size of 18 μm (powder I) an increase in temperature from 300 to 630 °C leads to an increase in average particle velocity from 610 to 765 m/s. Furthermore, an increase in spray temperature leads to an increase in particle temperature that is estimated from:

$$T = \frac{T_o}{1 + M^2(\gamma - 1)/2} \quad \text{(Eq 4)}$$

where T is the gas temperature (°C), T_o is stagnation temperature in the nozzle (°C) and M is the Mach number. It is worth noting that Eq 4 is applied in respect to this assumption that the distance between the nozzle exit and substrate is small, and therefore the particle temperature between the nozzle exit and substrate (before deposition) remains constant.

The outcome of Eq 4 for powder I (particle size distribution) at 300 °C is shown in Fig. 9. The figure shows that the temperature for the largest particles (e.g., 62 μm) in powder I is 260 °C. This temperature is 20 °C higher than the temperature for 5 μm particles. This seems to be due to the longer exposure of the large (62 μm) particles to the gas stream due to their lower velocity compared with small (5 μm) particles. For instance, the velocity for 62 μm particles (at 300 °C) is 1200 m/s less than the velocity for 5 μm particles (Fig. 10).

The estimated results show that an increase in spray tempera-

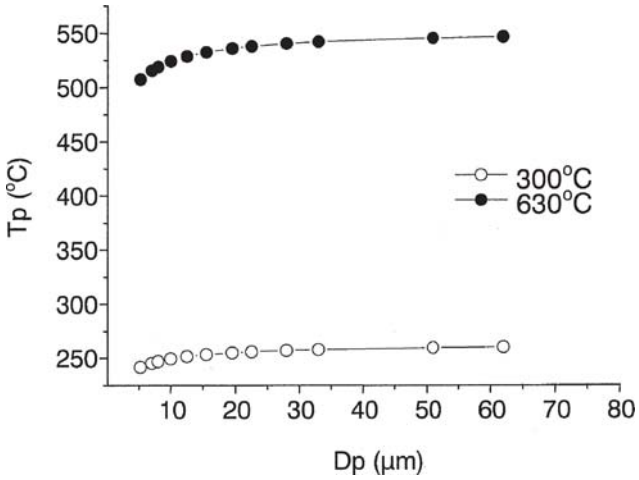

Fig. 9 Estimated particle temperature as a function of particle size (diameter) at 300 and 630 °C spray temperatures and 3 MPa spray pressure

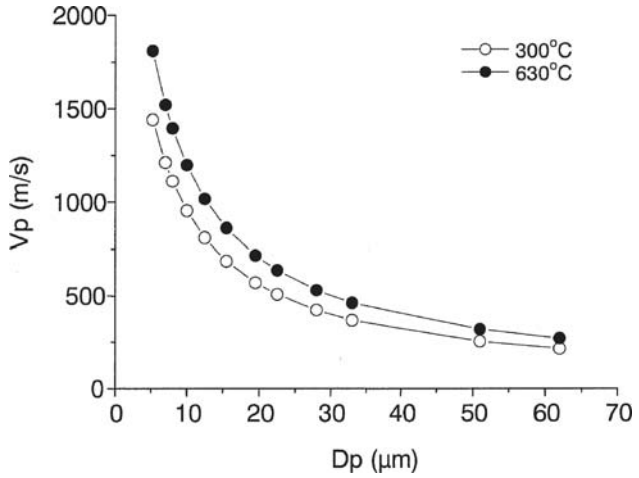

Fig. 10 Estimated particle velocity as a function of particle size at 300 and 630 °C cold spray temperature and 3 MPa cold spray pressure for powder I

ture from 300 to 630 °C leads to an almost uniform 270 °C increase in particle temperature. It is speculated that this increase in temperature has a profound effect on stress-strain behavior of deposited material at the moment of impact by decreasing the material resistance to shear flow. This means that particles lose their shear strength and undergo excessive deformation, which results in elimination of the porosities. Furthermore, a higher plastic deformation is expected for small particles (i.e., 5 μm) at 630 °C compared with 300 °C due to 300 m/s higher velocity that provides the required energy for significant deformation (Fig. 10).

Overall, it seems that the effect of spray temperature for elimination of porosity is more profound with respect to particle temperature compared with particle velocity. This is explained by estimation of the temperature and velocity for 5 μm particles of powder I. These particles are expected to achieve the highest velocity for deposition in powder I. For instance, an increase in

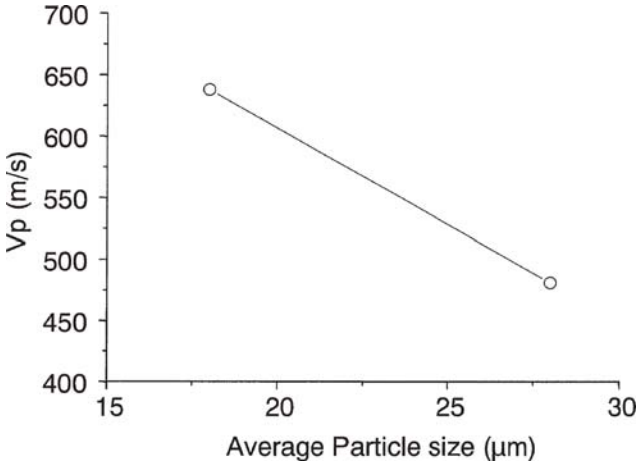

Fig. 11 Estimated particle velocity as a function of average particle size for powder I (18 μm) and powder II (28 μm) at 300 °C spray temperature and 3 MPa spray pressure

spray temperature from 300 to 630 °C results in an increase in particle velocity by 24% from 1450 to 1800 m/s. However, Fig. 9 reveals that for the same spray conditions temperatures of these particles increase from 240 to 510 °C (112%). This suggests that the particle temperature may play a more significant role in deposition of dense coatings compared with particle velocity. This is a complicated issue because it involves the relationship between the mechanical properties (i.e., stress-strain behavior) of particles and cold spray parameters that is not well established. Further study is required to quantify the relationship between the spray temperature and plastic deformation required to control porosity formation in the cold spray process.

4.2 Effect of Pressure

In contrast to spray temperature that influences particle speed, it has been proposed that spray pressure (under Mach condition) mostly affects particle acceleration (Ref 8, 10). Figure 7 shows that an increase in spray pressure from 2 to 3 MPa (20 to 30 bar) led to a 60% decline in volume fraction of porosity from 1 to 0.4% for powder I. For the same travel distance (e.g., standoff), a lower acceleration of particles at 2 MPa results in particles acquiring a lower velocity compared with 3 MPa spray pressure. Under these conditions, a higher volume fraction of porosity is expected at 2 MPa pressure (Fig. 7a) due to the lower velocity and therefore less plastic deformation of particles. Further study is required to quantify the relationship between the pressure and acceleration of the particles.

4.3 Effect of Particle Size

Results show that an increase in the average particle size from 18 to 28 μm leads to an increase in volume fraction of porosity from 0.7 to 1.5% (Fig. 8a). This is most likely due to the fact that large particles did not acquire the required velocity (and kinetic energy) for plastic deformation. For instance, the average velocity for powder II particles with larger average particle size is 165 m/s less than powder I particles (Fig. 11). It is worth noting that the above analysis for powders I and II were made with

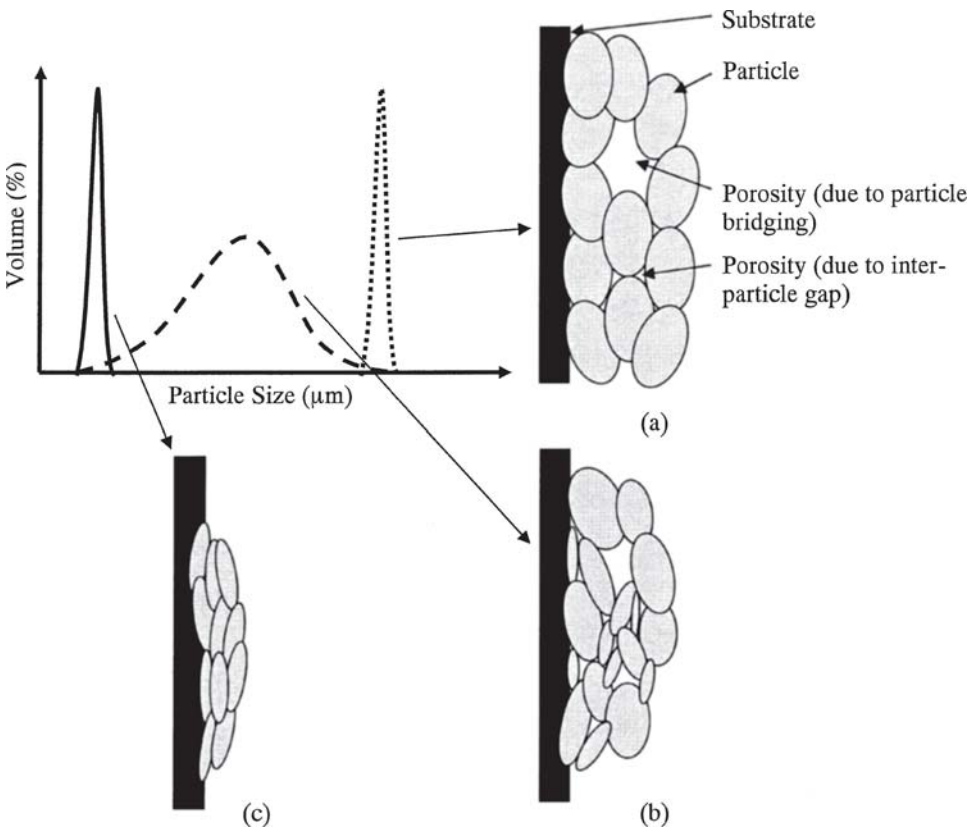

Fig. 12 Effect of powder of (a) large particle size and a narrow particle size distribution, (b) a mixture of small and large particle size with a broad particle size distribution, and (c) a small particle size with a narrow particle size distribution on porosity formation in cold spray process

respect to the average particle size to make a quantitative relationship with porosity. However, size distribution of particles (Fig. 2) is equally important for porosity formation.

A schematic representation of the particle size distribution effect on porosity formation is presented in Fig. 12. Three powder size distributions are presented: (a) a powder with a large particle size and a narrow particle size distribution, (b) a powder with a mixture of small and large particles that represents a broad particle size distribution, and (c) a small particle size powder with a narrow particle size distribution. The term "narrow particle size distribution" defines an ideal condition in which particles are almost the same size in the powder. Similarly, the term "broad particle size distribution" represents a range (a mixture of small and large particles) for particle size in the powder (Fig. 12).

In the ideal case (a), large particles hardly achieve the gas stream velocity and therefore a limited plastic deformation (flattening) occurs. However, these particles may achieve the required velocity for deposition. In this condition, the cold spray coating exhibits porosities in the microstructure that may develop due to interparticle gaps and bridging of the particles (Fig. 12a). Under the conditions that a mixture of large and small particles deposit, case (b), small particles acquire enough velocity (kinetic energy) to deform significantly (Fig. 12b). However, the large particles (similar to the schematic in Fig. 12a) do not considerably deform. This results in a heterogeneous porosity formation with small and large cavities. In the last case (c) small particles achieve the maximum velocity (in the gas stream) required for particles to significantly deform and eliminate voids between particles. This leads to a considerable reduction in volume fraction of porosity and the average porosity size (Fig. 12c).

In general, powders produced for industrial applications exhibit a broad particle size distribution (Fig. 2 and 12b), which makes determination of the particles velocity difficult. For powders of this study the velocity distribution of particles is shown in Fig. 13, estimated from Eq 2. The figure shows that at a spray temperature of 300 °C, the largest particles of powder II (i.e., 110 μm) cannot achieve the critical velocity required for deposition. This velocity is estimated from (Ref 9):

$$V_{cr} = 667 - 14\rho + 0.08T_m + 0.1\sigma_u - 0.4T_p \quad \text{(Eq 5)}$$

where V_{cr} is the critical velocity for deposition, ρ is the density (g/cm^3), T_m is melting temperature (°C), σ_u is the ultimate tensile strength (MPa), and T_p is the initial particle temperature (°C). Equation 5 yields the estimated V_{cr} for powder I (pure copper) with 1100 °C melting temperature, ultimate tensile strength of 220 MPa, and particle temperature estimated from Eq 3 to be 550 m/s. This estimated velocity is consistent with previous findings in the literature (Ref 9). Figure 13 reveals that only particles below 20 μm for powder I deposit during the spray process. A similar result is obtained for powder II. However, it is speculated that a higher volume of large particles (>20 μm) in

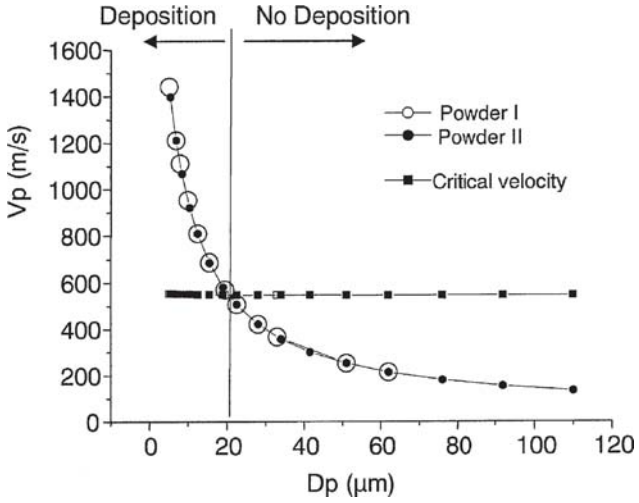

Fig. 13 Estimated velocity of the particles of powders I and II compared with the critical velocity for deposition at 300 °C and 3 MPa cold spray conditions

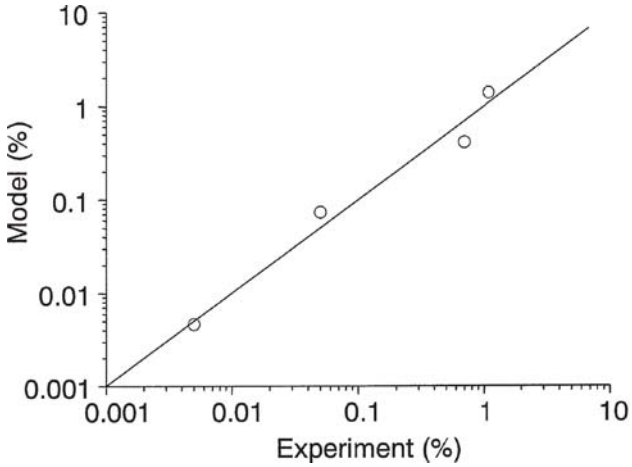

Fig. 14 Comparison of the model and experimental results for estimation of the volume fraction of porosity for alloy of this study

powder II results in a lower deposition efficiency compared with powder I (Fig. 2 and 13).

4.4 Model for Porosity

The above results demonstrate that particle temperature and particle velocity are the most important variables with respect to porosity formation. In this respect, the volume fraction of porosity as a (multiple linear regression) function of these variables is estimated from:

$$\log (Vol_p) = 11.66 - 2.2 \log (T_p V_p) + 4 \times 10^{-6} T_p V_p \qquad \text{(Eq 6)}$$

where Vol_p is the volume fraction of porosity (%), T_p is particle temperature (°C), and V_p is the particle velocity corresponding to average particle size (m/s). A linear least squares fit of the estimated volume fraction of porosity using Eq 6 shows very good agreement with experimental data (Fig. 14).

Overall, it seems that control over porosity during deposition has a significant role in utilization of cold spray for a range of industrial applications. For example, when a coating with a homogenous porosity is required (such as biomaterials and membranes) a powder with a narrow and large particle size could be used. Furthermore, cold spray conditions should be optimized in such a way that satisfies the conditions for critical velocity for deposition in Eq 4. This results in a porous coating in that particles deposit but do not deform significantly.

In contrast, for a dense and compact cold spray coating (i.e., high strength, corrosion resistant, and high thermal conductivity) particles must deposit at elevated temperatures and higher velocity. In this respect, a powder with a small particle size and narrow particle size distribution is beneficial. It appears that the critical condition that leads to elimination of porosity is a strong function of particle temperature, particle velocity, and particle mechanical properties (i.e., stress strain behavior). However, the relationships between these parameters and porosity formation have not been systematically studied and further study is needed.

5. Conclusions

Control over the porosity formation in cold spray coating provides the potential for application of this process to a wide range of industrial applications from porous to high-density materials. In this study, the effects of temperature, pressure, and particle size with respect to porosity formation in the cold spray process were evaluated. It was observed that an increase in spray temperature from 300 to 630 °C results in a decrease in the volume fraction of porosity from 44 to 2.5 μm. Similarly, an increase in temperature leads to a decline in average size of porosities. These are due to the fact that an increase in spray temperature increases the particle velocity and the particle temperature. The outcome of this study shows that particle temperature has a profound effect on porosity elimination. Furthermore, it was shown that a powder with a small particle size and a narrow particle size distribution is preferable for deposition of dense cold spray copper coatings. In contrast, a large particle size powder is beneficial for formation of a porous coating.

References

1. A.P. Alkhimov, A.N. Papyrin, V.P. Dosarev, N.J. Nesterovich, and M.M. Shuspanov, "Gas-Dynamic Spray Method for Applying a Coating," U.S. Patent 5,302,414, April 12, 1994
2. R.C. McCune, A.N. Papyrin, J.N. Hall, W.L. Riggs II, and P.H. Zajchowski, An Exploration of the Cold Gas-Dynamic Spray Method for Several Materials Systems, *Advances in Thermal Spray Science & Technology,* C.C. Berndt and S. Sampath, Ed., Sept 11-15, 1995 (Houston, TX), ASM International, 1995, 774 pages
3. D.L. Gilmore, R.C. Dykhuizen, R.A. Neiser, T.J. Roemer, and M.F. Smith, Particle Velocity and Deposition Efficiency in the Cold Spray Process, *J. Therm. Spray Technol.,* 1999, **8**(4), p 576-582
4. R.C. McCune, W.T. Donlon, E.L. Cartwright, A.N. Papyrin, E.F. Rybicki, and J.R. Shadley, Characterization of Copper and Steel Coatings Made by the Cold Gas-Dynamic Spray Method, *Thermal Spray: Practical Solutions for Engineering Problems,* C.C. Berndt, Ed., ASM International, 1996, p 397-403
5. T.H. Van Steenkiste, J.R. Smith, and R.E. Teets, Aluminium Coatings via Kinetic Spray with Relatively Large Powder Particles, *Surf. Coat. Technol.,* 2002, **154**(2), p 237-252
6. J. Karthikeyan, C.M. Kay, J. Lindeman, R.S. Lima, and C.C. Berndt, Cold Spray Processing of Titanium Powder, *Thermal Spray: Surface*

Engineering via Applied Research, C.C. Berndt, Ed., May 8-11, 2000 (Montreal, Quebec, Canada), ASM International, 2000, 1383 pages
7. T. Van Steenkiste and J.R. Smith, Evaluation of Coatings Produced via Kinetic and Cold Spray Processes, *J. Therm. Spray Technol.,* 2004, **13**(2), p 274-282
8. R.C. Dykhuizen and M.F. Smith, Gas Dynamic Principles of Cold Spray, *J. Therm. Spray Technol.,* 1998, **7**(2), p 205-212
9. H. Assadi, F. Gärtner, T. Stoltenhoff, and H. Kreye, Bonding Mechanism in Cold Gas Spraying, *Acta Mater.,* 2003, **51**(15), p 4379-4394
10. T. Stoltenhoff, H. Kreye, and H.J. Richter, An Analysis of the Cold Spray Process and Its Coatings, *J. Therm. Spray Technol.,* 2002, **11**(4), p 542-550
11. R. Morgan, P. Fox, J. Pattison, C. Sutcliffe, and W. O'Neill, Analysis of Cold Gas Dynamically Sprayed Aluminium Deposits, *Mater. Lett.,* 2004, **58,** p 1317-1320
12. A.N. Papyrin, S.V. Klinkov, and V.F. Kosarev, Modeling of Particle-Substrate Adhesive Interaction under the Cold Spray Process, *Thermal Spray 2003: Advancing the Science & Applying the Technology,* B.R. Marple and C. Moreau, Ed., ASM International, 2003, Vol 1: 845 pages; Vol 2: 864 pages
13. J. Vlcek, L. Gimeno, H. Huber, and E. Lugscheider, A Systematic Approach to Material Eligibility for the Cold Spray Processes, *Mater. Lett.,* 2004, **58,** p 37-44.
14. R.S. Lima, J. Karthikeyan, C.M. Kay, J. Lindemann, and C.C. Berndt, Microstructural Characteristics of Cold-Sprayed Nanostructured WC-Co Coatings, *Thin Solid Films,* 2002, **416,** p 129-135